Supporting Information

S1. The structural analysis of monoclinic VO_2 (M) and tetragonal rutile VO_2 (R).

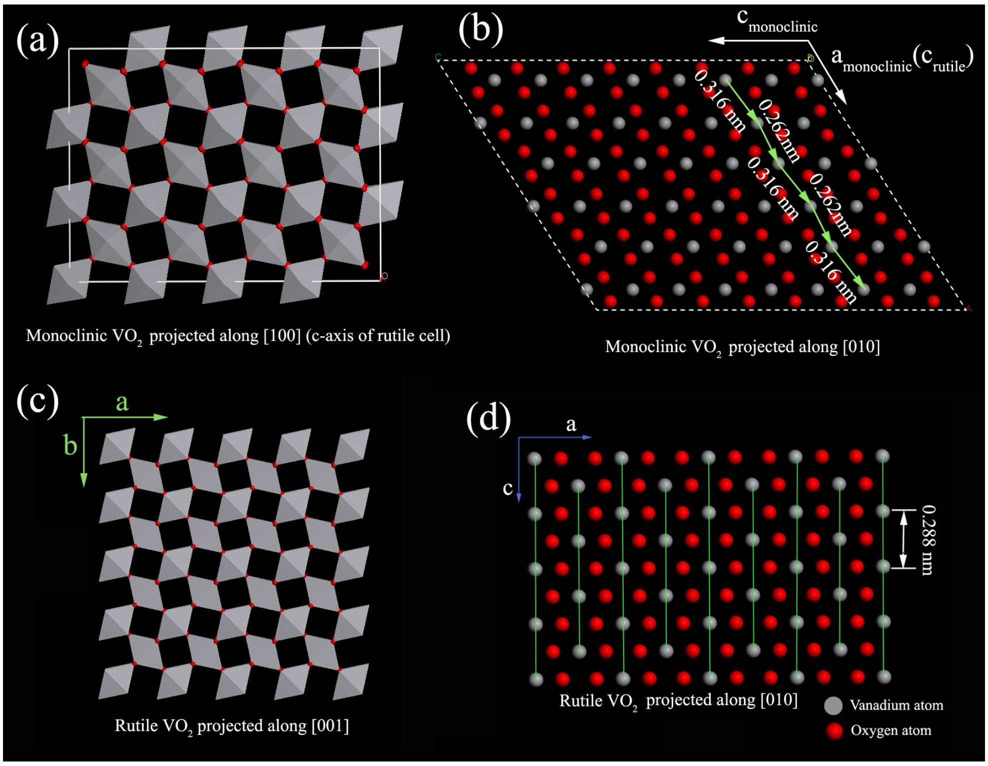

Figure S1. (a-b) monoclinic VO_2 (M) structure: (a) Crystal structure of monoclinic VO_2 (M) projected along [100] (c-axis of rutile cell). (b) The super-cell structure of monoclinic VO_2 (M) projected along [010], where the distortion of vanadium atom was clearly seen by the green color arrows along the a-axis (c-axis of rutile cell). For monoclinic VO_2 (M), the presence of two different V-V distances of 0.262 and 0.316 nm between the nearest vanadium atoms of the zigzag-type vanadium atom chains along the c_R-axis, leads to the localization of d-orbit electrons to give insulator behavior of monoclinic VO_2.[1] **(c-d) Rutile VO_2 (R) structure:** (c) Crystal structure of tetragonal rutile VO_2 (R) projected along [001]; (d) The super-cell structure of rutile VO_2 (R) projected along [010], and vanadium atoms built chains parallel to the c axis of the structure. For rutile VO_2(R), the presence of infinite chains along the rutile c-axis (c_R-axis) with the nearest neighboring V-V distance of 0.288 nm leads to the d-orbit electrons share by all of the metal V atoms, giving the metallic behavior of VO_2(R).[2]

S2. XPS characterization of the as-obtained monoclinic VO_2(M) nanorods

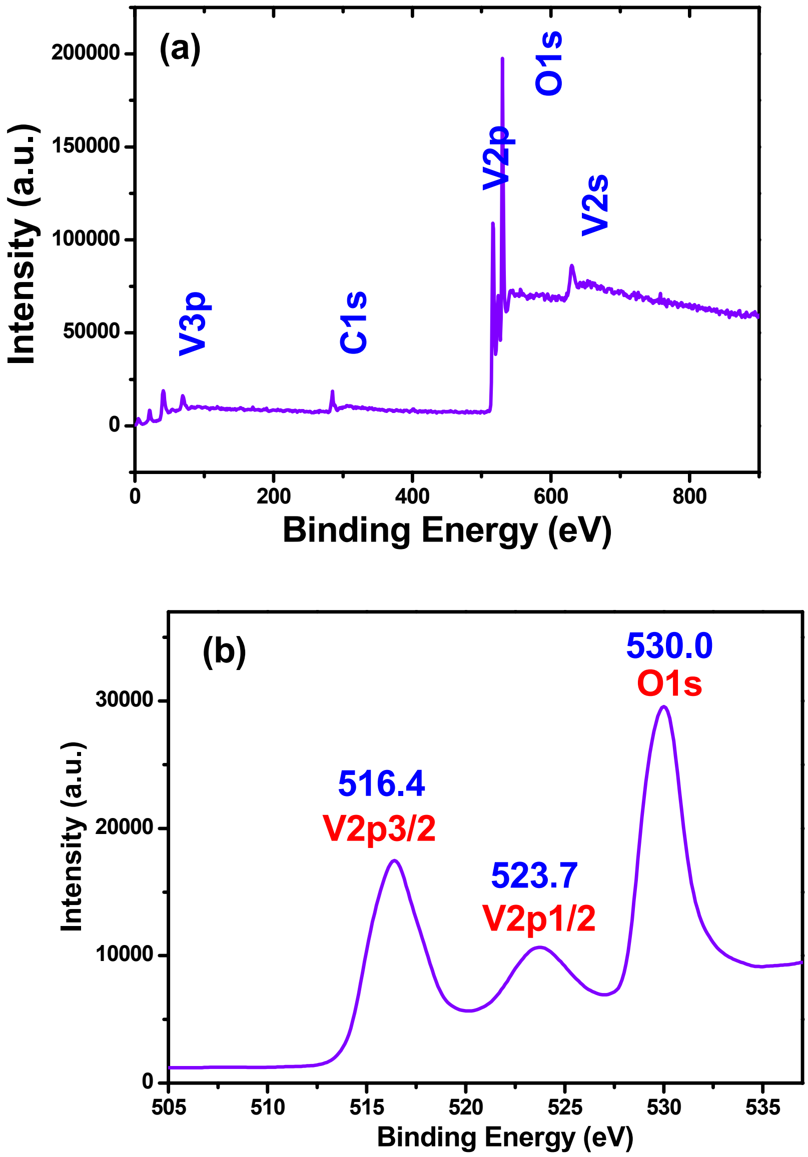

Figure S2. (a) The survey XPS spectrum of synthetic monoclinic VO_2(M) product, where only the V and O can be found while the carbon peak at 284.6 eV was taken as reference. (b) the high resolution XPS (HRXPS) for V2p and O1s region.

The direct information for the valence state of vanadium ions can be provided by the analysis of the surface molecular and electronic structure of the products by XPS as shown in **Figure S2**, where the average atomic ratio of V and O is 1:2.01 on the basis of the quantification of V_{2p} and O_{1s} peaks. High resolution XPS (HRXPS) for O_{1s} region (inset in **Figure S2b**) shows an symmetry core level centered at 530.0 eV that can be assigned to the O^{2-} in the V-O [3], which well accords with the structural information in VO_2(M) structure. Also, the V_{2p} core level spectrum (**Figure S2b**) illustrates that the observed value (516.4 eV) of the binding energies for $V_{2p3/2}$ is in agreement with the literature values of bulk for V^{4+} [4, 5]. In addition, the difference in binding energy (Δ) between the O1s and $V2p_{3/2}$ level could also be used to determine the oxidation state of the vanadium oxides [6]. Here, Δ value of VO_2(M) sample is 13.6 eV, approaching the reported value in the literature for V^{4+} [7, 8].

S3. Size distribution histograms of the as-obtained monoclinic VO_2(M) nanorods

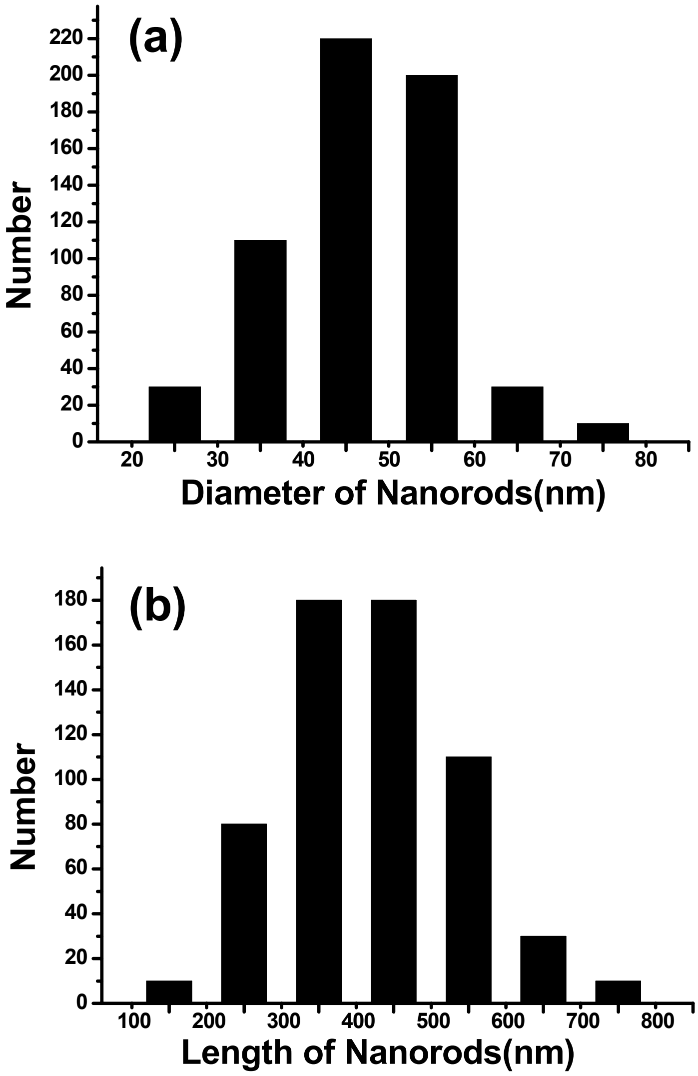

Figure S3. The diameter and length size distribution histogram of the as-obtained nanorods for monoclinic VO_2(M), showing that the nanorod outlook with the diameter size ranging from 30 nm to 120 nm and lengths up to 400 - 800 nm in large scale.

S4. SAED pattern analysis

The angle values between the selected lattice planes provides the evidence for the existence of monoclinic VO_2 in the solution synthesis conditions. The experimental angle value for the selected lattice planes was directly determined by the corresponding angle between the two lines, in which the two lines were formed by the linkage of each of two selected points (representing the concerned two lattice planes (*h1, k1, l1*) and (*h2, k2, l2*)) with the zone-axis point in the same SAED pattern, respectively.

On the other hand, the theoretical angle value was obtained by the crystallographic parameters calculation based on the monoclinic VO_2(M) crystal parameters. As is known, for a typical monoclinic lattices, the parameter relationship for the monoclinic cell should obey the following formula: $a \neq b \neq c$, $\alpha = \gamma = 90^o$, $\beta \neq 90^o$. Moreover, the interplaner spacing value for two selected crystal planes (*h1, k1, l1*) and (*h2, k2, l2*), their theoretical angle can be given based on the following formula:

$$\cos\varphi = \frac{\dfrac{h_1h_2}{a^2\sin^2\beta}+\dfrac{k_1k_2}{b^2}+\dfrac{l_1l_2}{c^2\sin^2\beta}-\dfrac{(h_1l_2+l_1h_2)\cos\beta}{ac\sin^2\beta}}{\left[\left(\dfrac{h_1^2}{a^2\sin^2\beta}+\dfrac{k_1^2}{b^2}+\dfrac{l_1^2}{c^2\sin^2\beta}-\dfrac{2h_1l_1\cos\beta}{ac\sin^2\beta}\right)\cdot\left(\dfrac{h_2^2}{a^2\sin^2\beta}+\dfrac{k_2^2}{b^2}+\dfrac{l_2^2}{c^2\sin^2\beta}-\dfrac{2h_2l_2\cos\beta}{ac\sin^2\beta}\right)\right]^{1/2}} \qquad (2)$$

In our case, the experimental and calculation angle value results were summarized in **Table S4**. Note that all the lattice planes were taken from the SARD patterns in Figure 2. Based on our analysis results, the experimental angle values agree well with the corresponding calculated ones, giving the solid evidence that the as-obtained sample was indeed monoclinic VO_2(M).

Table S4. The summary information of the experimental angle values and the theoretical angle values for the as-obtained monoclinic VO_2(M).

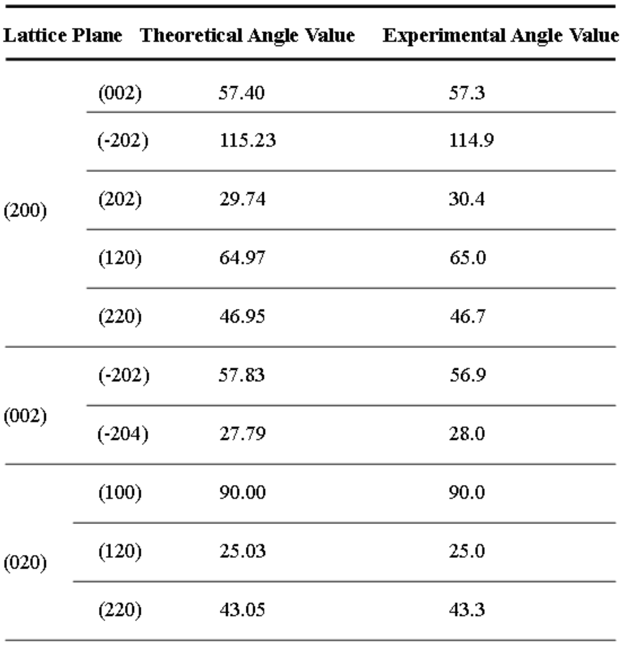

Lattice Plane		Theoretical Angle Value	Experimental Angle Value
(200)	(002)	57.40	57.3
	(-202)	115.23	114.9
	(202)	29.74	30.4
	(120)	64.97	65.0
	(220)	46.95	46.7
(002)	(-202)	57.83	56.9
	(-204)	27.79	28.0
(020)	(100)	90.00	90.0
	(120)	25.03	25.0
	(220)	43.05	43.3

S5. The summary information of the comparison experiments

Table S5. The summary information of the comparison experiments using different vanadium sources and different amount of HNO_3 amount keeping other reaction parameters constant.

Vanadium sources		Oxidant / Reductant	Product
V^{5+}	V_2O_5	Ethylene glycol	VO_2(B) ^{Note1}
	NH_4VO_3	HCOOH	VO_2(B) ^{Note2}
	Na_3VO_4	HCOOH	VO_2(B)
V^{4+}	VO(acac)$_2$	None	VO_2(B)^{Note3}
	$VOSO_4$	None	VO_2(B)^{Note4}
$V(OH)_2NH_2$		0 mL 0.1 M HNO_3	Lepidocrocite VOOH
		2.5 mL 0.1 M HNO_3	Unknown phase
		3.5 mL 0.1 M HNO_3	VO_2(M)
		4.0 mL 0.1 M HNO_3	$VO_2(M)+H_2V_3O_8$
		4.5 mL 0.1 M HNO_3	$VO_2(M)+H_2V_3O_8$
		5.0 mL 0.1 M HNO_3	$VO_2(M)+H_2V_3O_8$
		5.5 mL 0.1 M HNO_3	$H_2V_3O_8$

Note: 1. X.Y. Chen, X. Wang, Z.H. Wang, J.X. Wan, J.W. Liu, Y.T. Qian Nanotech. 2004, 15, 1685.

2. J.F. Liu, Q.H. Li, T.H. Wang, D.P. Yu, Y.D. Li Angew. Chem. Int. Ed. 2004, 43, 5048.
3. S.D. Zhang, Y.M. Li, C.Z. Wu, F. Zheng, Y. Xie J. Phys. Chem. C 2009, 113, 15058.
4. F Zhou, X M Zhao, H Xu et al. Chem. Lett., 2006, 35(11): 1280~1281.
5. Other chemical reagents such as VO(acac)$_2$ were purchased from from Alfa Aesar. And Na_3VO_4, HNO_3, HCOOH were purchased from Sinopharm Chemical Reagent Co., LtdS in Shanghai city.

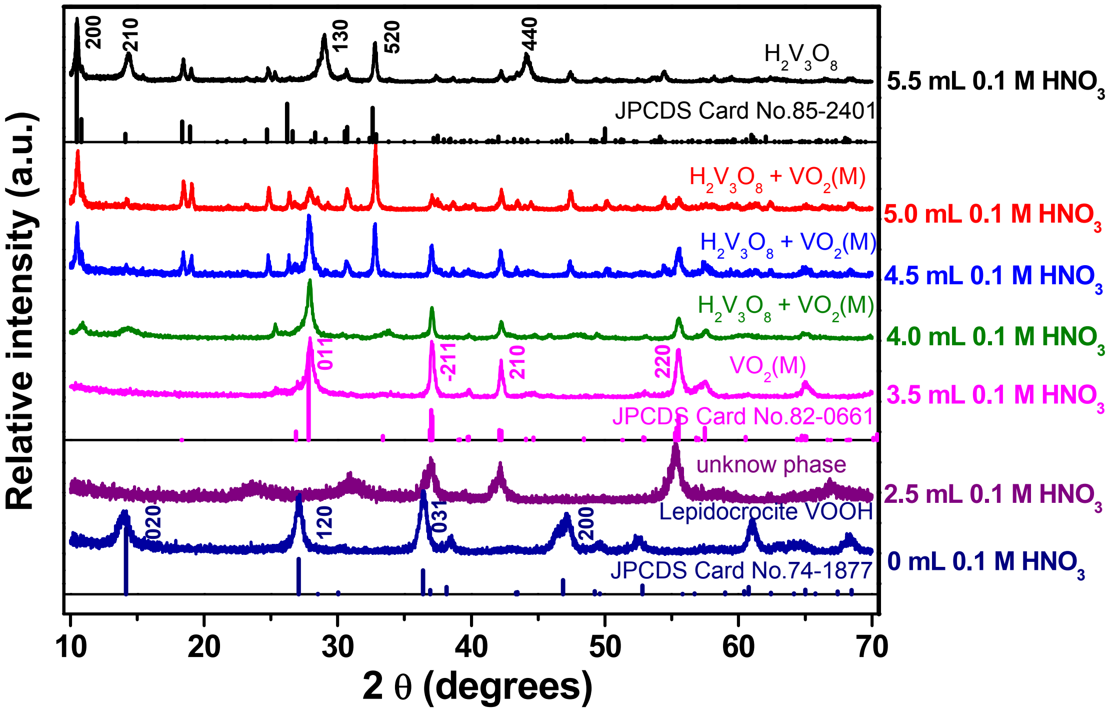

Figure S5. XRD patterns of the as-obtained samples when different amount of HNO_3 was involved keeping other reaction parameters constant.

References

[1] S. Biermann, A. Poteryaev, A. I. Lichtenstein, A. Georges, *Phys. Rev. Lett.* 2005, ***94***, 026404.

[2] C. Z. Wu, J. Dai, X. D. Zhang, J. L. Yang, Y. Xie, *J. Am. Chem. Soc.* 2009, ***131***, 7218.

[3] G. Silversmit, D. Depla, H. Poelman, G. B. Marin, R. De Gryse, *J. Electro. Spectro. Relat. Pheno.* 2004, ***135***, 167.

[4] G. A. Sawatzky, D. Post, *Phys. Rev. B* 1979, ***20***, 1546.

[5] C. Z. Wu, Z. P. Hu, W. Wang, M. A. Zhang, J. L. Yang, Y. Xie, *Chem. Comm.* 2008, 3891.

[6] J. Mendialdua, R. Casanova, Y. Barbaux, *J. Electro. Spectro. Rel. Pheno.* 1995, ***71***, 249.

[7] F. Werfel, G. Drager, U. Berg, *Cryst. Res. Tech.* 1981, ***16***, 119.

[8] C. Z. Wu, Y. Xie, L. Y. Lei, S. Q. Hu, C. Z. OuYang, *Adv. Mater.* 2006, ***18***, 1727.